Design Optimization Considering a Detailed PCB Stator Layout for Coreless AFPM Machines with Minimal Eddy and Circulating Current Losses

Yaser Chulaee[1], Greg Heins[2], Ben Robinson[2], Mark Theile[2], Dean Patterson[2], Dan M. Ionel[1]

[1]SPARK Laboratory, Stanley and Karen Pigman College of Engineering, University of Kentucky, Lexington, KY, USA
[2]Regal Rexnord Corp., Research and Development, Rowville, VIC, Australia

yaser.chulaee@uky.edu, greg.heins@ieee.org, ben.robinson@regalrexnord.com, mark.thiele@regalrexnord.com, dean.patterson@ieee.org, dan.ionel@ieee.org

Abstract—**This paper proposes a multi-objective design optimization approach for printed circuit board (PCB) stator coreless axial flux permanent magnet (AFPM) machines based on a detailed PCB stator layout. The process begins with the machine envelope design optimization based on an evolutionary algorithm and 3D finite element analysis (FEA) models and continues with the detailed design of a PCB stator aimed at minimizing eddy and circulating current losses. This approach employs different open circuit loss mitigation techniques while taking into account PCB manufacturing limitations and standards. The process is explained through the design of an integral horsepower PCB stator coreless AFPM machine, which was prototyped and tested. The experimental results indicate negligible open circuit losses and 96% efficiency at the speed of 2,100rpm and an output torque of 19Nm, thereby validating the efficacy of the proposed approach.**

Index Terms—**Axial-flux, coreless machines, FEA, optimization, differential evolution, permanent-magnet machines, PCB stator, winding losses, eddy current, circulating current.**

I. Introduction

Axial flux permanent magnet (AFPM) synchronous machines are gaining popularity in various applications, such as HVAC systems, aviation propulsion, and electric vehicles [1]. The coreless (air-cored) stator AFPM machine topology offers notable advantages over conventional designs by eliminating magnetic cores and their associated losses, including the absence of cogging torque, reduced audible noise and vibration, as well as decreased weight and volume. These features collectively contribute to an increase in efficiency and specific torque (Nm/kg) [2, 3].

Currently, designers are confronted with the challenge of mitigating stator winding losses, which serve as the primary source of loss in coreless machines. In this type of machine, where there is no magnetic core in the stator, the copper conductors are directly exposed to fluctuations in the airgap's magnetic flux density. This exposure can lead to considerable losses caused by eddy currents [4, 5]. Furthermore, machines with a wide magnetic airgap suffer from an uneven distribution of magnetic flux density and notable flux fringing. Consequently, parallel conductors experience varying induced voltages, resulting in circulating current losses [6, 7].

Lack of a magnetic core presents an opportunity to incorporate printed circuit board (PCB) stators in coreless AFPM machines, which have gained popularity due to their potentially more reliable and highly repeatable fabrication process, high modularity, and lightweight nature [8]. The significant flexibility in PCB coil shape design and their interconnections, with minimal impact on manufacturing setup, presents an excellent opportunity to enhance the efficiency of coreless machines through optimized stator coil designs. As a result, there has been a surge of studies focusing on the design and optimization of PCB coils with the primary objective of minimizing losses. [5, 9, 10].

The primary obstacle lies in the fact that many of the desired outcomes, such as minimizing eddy and circulating current losses, are contradictory and cannot be prioritized exclusively. Therefore, a systematic approach is imperative in designing such motors, which comprehensively considers all stator loss components and the trade-offs between them, while taking into account fabrication limitations and adhering to industry standards. This approach is vital for achieving high efficiency and unlocking the full potential of PCB stator coreless AFPM machines.

A detailed discussion of the trade-off between stator power loss components, including eddy current losses, circulating current losses, and DC copper losses, was presented in [7]. Moreover, a systematic guideline for mitigating these losses while considering typical PCB manufacturing limitations and standards is also proposed in this research. The authors studied and compared five different PCB windings, namely concentric, radial, arc, parallel, and unequal width, in [9]. A novel unequal-width parallel winding is also proposed and compared with parallel winding, which results in a 17% smaller phase resistance than parallel winding. The modeling and design procedure of a high-speed 1kW PCB coreless multi-phase AFPM machine with non-overlapped windings considering latest standards in the PCB manufacturing process, was proposed in [11]. A framework for the design and analysis of a commercially available axial flux permanent magnet motor with a coreless PCB stator and fully integrated variable
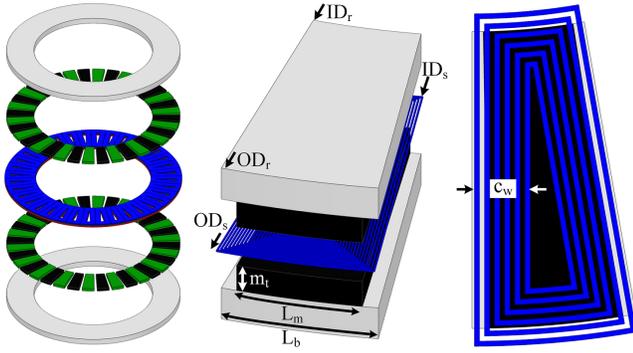
Var.	Description	Min	Max
g	airgap [mm]	0.75	1.50
k_{sr}	stator split ratio = $\frac{ID_s}{OD_s}$	0.65	0.85
k_{oh}	overhang ratio = $\frac{(OD_r - ID_r)}{(OD_s - ID_s)}$	0.57	1.00
c_w	coil width [mm]	7.00	9.00
k_m	PM coverage ratio = $\frac{L_m}{L_b}$	0.80	1.00
m_t	PM thickness [mm]	3.00	7.00
s_t	stator thickness [mm] (single phase)	1.12	3.00

Fig. 1. The exploded view of the machine configuration and the 3D FEA parametric model of one pole of the machine with the simplified PCB coil that was employed in the design optimization study.

frequency was presented by the authors in [12].

This paper proposes a multi-objective design optimization approach for PCB stator coreless AFPM (Axial Flux Permanent Magnet) machines, taking into account various components of stator windings loss. The design procedure consists of two main stages. First, an optimization study is conducted to minimize DC copper losses and magnet weight in the machine envelope. Subsequently, the focus shifts to designing the PCB stator coil, aiming to minimize eddy and circulating current losses while considering a detailed PCB layout. An exemplary highly efficient integral horsepower PCB stator coreless AFPM machine is specifically designed using this approach, showcasing the effectiveness of the process. All FEA (Finite Element Analysis) results are obtained from 3D models created in Ansys Electronics Desktop, utilizing the transient solution type [13, 14]. Furthermore, a physical prototype of the machine is fabricated, and its performance is evaluated through experimental tests.

II. PROBLEM FORMULATION AND DESIGN OPTIMIZATION

The designed machine must meet the specific application requirements, necessitating the delivery of a rated torque of 19Nm at 2,100rpm while maintaining a fixed total outer diameter of 310mm. The other geometrical variables and the number of pole pairs are investigated to attain the optimum design. AFPM machines have various configurations, and among them, the dual rotor single-stator design is prevalent because of its robustness and high torque density [12]. The exploded view of this configuration is demonstrated in Fig. 1. Manufacturers and customers prioritize cost competitiveness and efficiency when considering AFPM machines [15]. Therefore, the first step in this process is optimizing the machine envelope to minimize magnet weight, which has a significant impact on the machine's total cost, and DC copper losses. For this optimization study, a 3D parametric single-pole FEA model of the machine is employed, as shown in Fig. 1.

It should be noted that in this step, a simplified reduced-turn PCB coil that closely resembles the current density distribution of a real coil with a higher number of turns is utilized to considerably reduce the computational burden. The

real PCB coil will be designed in the next step based on the optimized coil envelope derived from the optimization process. In addition, all designs generate the same output torque by adjusting the current density, and to avoid saturation, the thickness of rotor back iron is also fixed at 10mm [16]. The design optimization process is fully automated through integrating Ansys and MATLAB by using scripting feature.

For this optimization study, seven geometrical independent variables are considered, as illustrated in Fig. 1 and listed in Table I. The outer diameter of the stator is set to 310mm and its inner diameter is determined by the stator split ratio, k_{sr}. The overhang ratio, represented by k_{oh}, governs the proportion of the magnet radial length to the stator coil radial length, and when k_{oh} is equal to one, the rotor magnets completely cover the end coil. In this study, a multi-objective differential evolution (MODE) optimization algorithm is employed to discover the Pareto front, i.e. optimal designs. The population size of each generation was set to 40 which is six times larger than the number of independent variables. If there is only a minor improvement in three selected points on the Pareto front for several consecutive generations, the optimization process is terminated. The search space for the optimal design is designated to be extensive, indicating that the optimization variables have wide ranges, with the sole exception of geometrical restrictions, which are implemented to avoid interference between different geometric components and to account for mechanical limitations such as minimum airgap and standard PCB thicknesses.

The design optimization process was concluded after 12 generations, during which 480 candidate designs were evaluated. All the designs and the Pareto set are demonstrated in Fig. 2. The normalized distributions of the optimization independent variables for the Pareto front designs are demonstrated as box plots in Fig. 3. Apart from the airgap, all the variables seem to be positioned comfortably far away from the bands, indicating that appropriate limits have been predetermined. It is also observed that the optimal designs within the Pareto front tend towards having a narrower airgap. Furthermore, the corresponding overhang ratio for each design is shown in Fig. 4 as a color code.

The results indicate that most of the relatively heavyweight designs with low copper losses have higher overhang ratios,
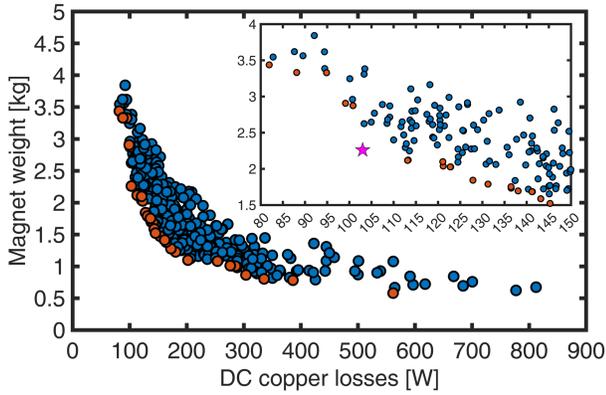
Fig. 2. All the designs evaluated in the optimization study, with the Pareto front shown as orange dots.

Fig. 3. Normalized distribution of the independent variables for the Pareto front designs.

meaning that rotor PMs cover the majority of the end coils. The end coil conductors not only do not contribute to torque generation but also increase the total eddy current losses due to variations in the airgap flux density. Therefore, it is not accurate to assume that designs with higher overhang ratios will have superior efficiencies. Designs that are positioned close to the knee point on the Pareto front have rotor PMs that partially encase the end coils. These designs exhibit lower eddy current losses while maintaining a favorable balance between magnet weight and DC copper losses.

Considering the rated specifications and taking into account manufacturing restrictions and standards, a preliminary calculation was conducted, and out of the designs that met the criteria of weighing less than 2.5kg and having DC copper losses under 150W, one was chosen for the subsequent stage of the design process. The selected design is marked by a star as shown in the zoomed-in view in Fig. 2. It should be noted that the copper losses of the actual coil can be derived by scaling the copper losses of the simplified coil with the ratio of slot fill factors (SFFs). A typical SFF of 0.18 for PCB coils based on previous research studies is considered for scaling at this stage [17, 18].

PCB manufacturing limitations and standards, as well as eddy current losses, are the main barriers to maximizing SFF and consequently reducing DC copper losses. As mentioned before, a simplified 3D FE model of the PCB coil with a thickness of s_t is considered for the coil envelope optimization. The DC copper losses of a single coil in terms of current density J in traces, and SFF can be written as:

$$P_{cu} = \frac{\rho . l_c . (N_L . N_t . I)^2}{A_c . SFF},$$ (1)

where A_c is the coil side cross section area and the number of turns per layer, the number of layers per coil, and the average length of the coil are denoted by N_t, N_L, and l_c, respectively. It is assumed that both the simplified and the actual coils have an equivalent ampere-turn, i.e., $(N_L . N_t . I)$ to produce the same output torque.

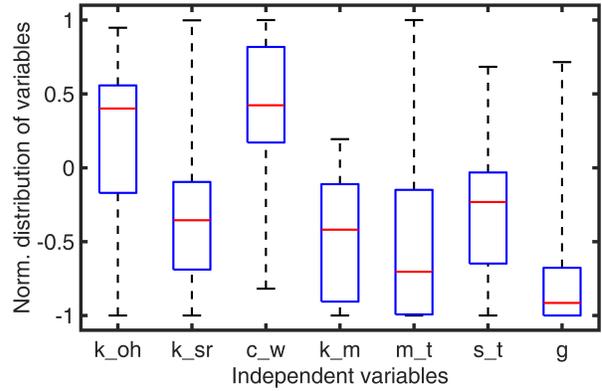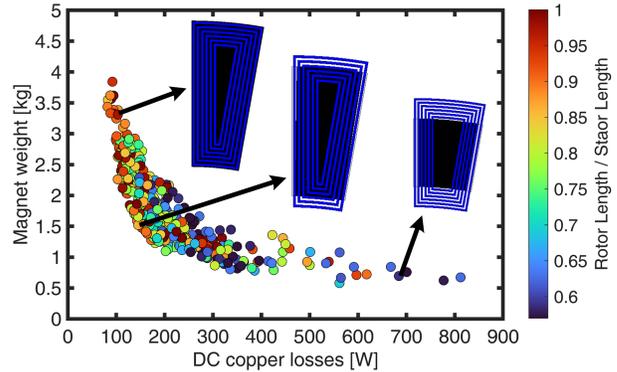Fig. 4. The overhang ratios, i.e., rotor length to stator length ratios, for all the designs within the optimization results are shown as color code.

III. PROPOSED SYSTEMATIC DESIGN PROCEDURE FOR A PCB STATOR

The next step focuses on designing the PCB stator in detail considering the given stator coil envelope of the selected design. In this process, the minimization of all stator loss components is considered simultaneously. The total eddy current losses within PCB traces with rectangular cross section can be calculated by:

$$P_{ed} = \frac{\pi^2 N_c N_t f^2 t_w t_h l_c}{6\rho} \left(t_w^2 B_z^2 + t_h^2 B_\phi^2 \right),$$ (2)

where N_c is number of coil sides with average length of l_c; and N_t the turns per coil; B_z and B_ϕ are axial and tangential components of the flux density, respectively; t_w the trace width; t_h the trace height, in the z direction; and f denotes the frequency of flux variations [7, 19]. This equation implies that the magnitude of eddy current losses is proportional to the cube of the trace width, emphasizing the minimization of trace width to avoid high eddy current losses.

The minimum trace width is limited by the PCB manufacturer's capabilities and standards. Moreover, decreasing the trace width has the disadvantage of lowering the SFF and the current-carrying capacity of the phase winding. As the tangential component of the airgap flux density B_ϕ, is
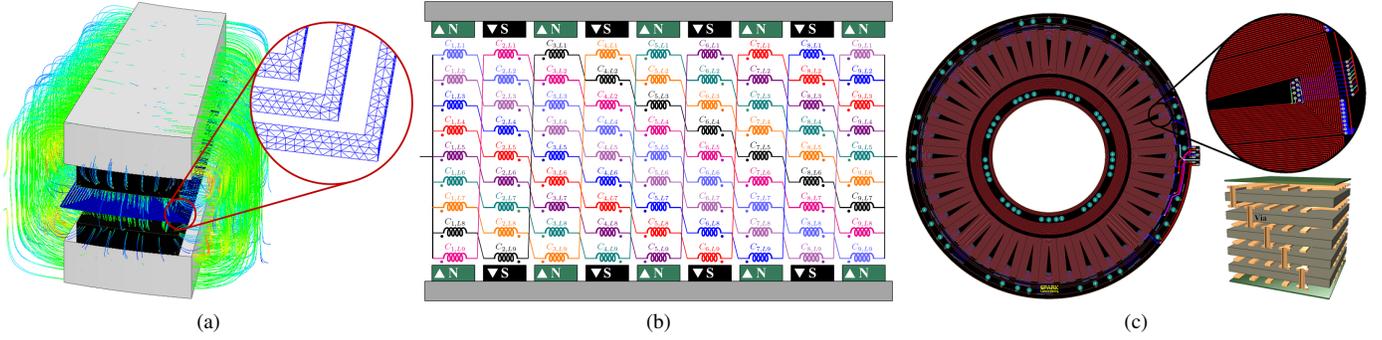
Fig. 5. Flux lines of the 3D FEA model and the very fine mesh elements on the designed PCB coil model for eddy current loss calculation (a). The complete layer transposition implementation for a 9-layer PCB stator with 9 coils in series (b). The designed 36-pole PCB stator with 9 active layers and one layer for other connections. Note the very narrow traces with a width of 0.22 mm, which greatly reduce eddy current losses (c).

insignificant, using relatively thick traces instead of wide traces improves SFF and current-carrying capacity with no considerable impact on eddy current losses. Implementing thick copper traces with a narrow width is challenging, and the minimum ratio, i.e., t_w/t_h, provided by the manufacturers has to be considered.

Another effective approach to improve current-carrying capability is to use multiple identical coils in different layers that are connected in parallel. The main challenge of this approach is that, due to the non-uniform airgap flux density in coreless AFPM machines and the fringing effect, axially distributed parallel coils experience a different magnetic flux, resulting in different induced voltages and consequently circulating current losses according to the following:

$$ P_{cr} = \sum_{i=1}^{n} RI_i^2 = \frac{1}{R} \sum_{i=1}^{n} \left[E_i - \frac{\sum_{i=1}^{n} E_i}{n} \right]^2. \quad (3) $$

This equation expresses the circulating current losses within n parallel paths with an equal resistance of R where the induced voltage of ith path is denoted by E_i [7].

A complete layer transposition is proposed in this paper as an effective technique to significantly mitigate circulating current losses between parallel strands. This transposition geometrically balances the back-EMFs by ensuring all paths in different layers are impacted equally by airgap flux density variation, creating similar induced voltages. This technique requires coordination between the number of parallel layers, coils in series, and poles for true and effective implementation. Thereby, in the stator design process, modification of various parameters, such as the number of pole pairs, is required until the design objectives are met. Further elaboration on this process will be provided subsequently.

The design of individual coils begins by choosing a trace width of 0.22mm, considering the required ampere-turn and maximum current carrying capability of PCB traces with natural air cooling and the design standard. It is worth mentioning that 0.22mm of trace width is close to the minimum limit for a copper thickness of 3oz (0.105mm). It should be noted that 3oz is the maximum copper weight allowed in a standard PCB manufacturing process. To fulfill the back-EMF
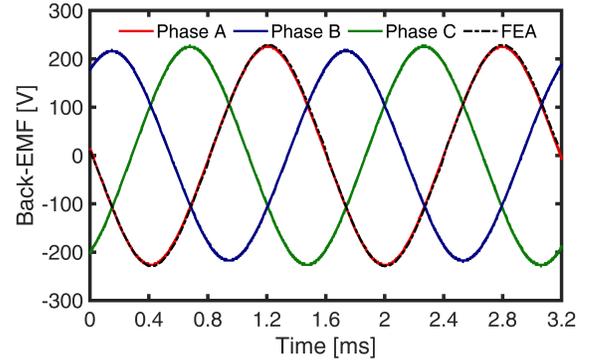

Fig. 6. The measured three-phase back-EMFs of the prototype machine, when compared with the results of the finite element analysis, show a very good agreement between the two sets of results.
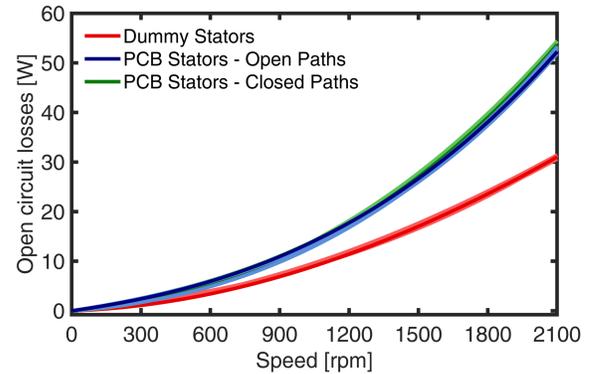

Fig. 7. Spindown tests results for measuring the mechanical and the stator open circuit losses. The eddy and circulating current losses are also separated by these experiments.

requirement at the rated speed with respect to the inverter DC-link, a total of 162 turns per phase are needed. For the given coil width without violating the minimum standard clearance between traces, nine coils in series, each with 18 turns, are considered. To improve the current-carrying capability of the stator windings, four sets of such coils are distributed around the stator and connected in parallel, resulting in a 36-pole stator. Due to the lack of high-frequency losses in the stator core, coreless machines can feature high polarity, resulting in
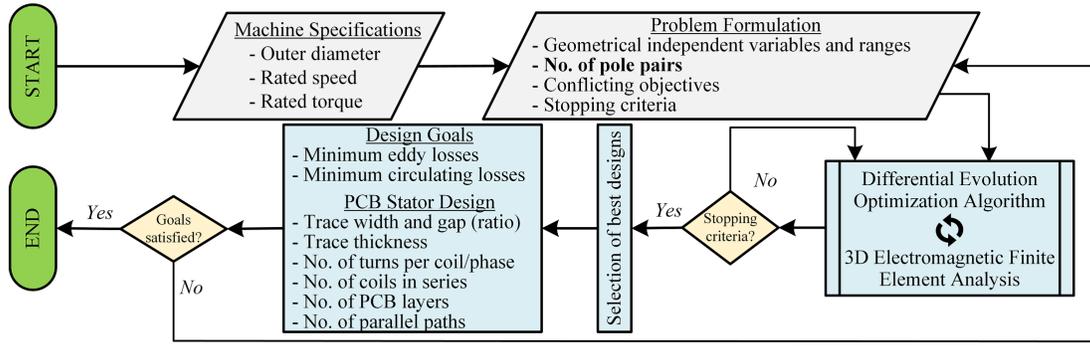
Fig. 8. The flowchart of the introduced multi-objective design optimization procedure for PCB stator coreless AFPM machines.

smoother operation and lower copper losses.

To prevent circulating current losses caused by the rotor abnormalities, the coils in different parallel paths are evenly distributed around the stator. Additionally, to further improve current-carrying capability, achieve a higher SFF, and eliminate the need for high current density in narrow PCB traces, a nine-layer PCB is considered. Therefore, the aforementioned pattern is repeated for nine layers, with each coil connected in parallel to the coil in the layer below it. The CAD model of the designed PCB stator for fabrication is also demonstrated in Fig. 5c. As mentioned before, circulating currents between axially distributed parallel connections can be significant.

A complete layer transposition is implemented within all coils to mitigate circulating current losses, as illustrated in Fig. 5b. The nine layer PCB between rotor magnets is expanded for the demonstration of connections between coils that are shown as inductors. This figure clearly shows that there must be a coordination between number of PCB layers in connected in parallel and coils connected in series to have a complete transposition. At this stage, if the number of pole pairs does not fulfill the other design considerations, one should return to the previous step and modify it accordingly. The 3D FEA model of the designed 18-turn coil used for eddy current calculations is depicted in Fig. 5a. The flowchart presented in Fig. 8 provides a summary of the complete design process.

IV. Prototype Machine, Experimental Validation, and Discussion

The designed machine was prototyped, and the effectiveness of the employed loss mitigation techniques was experimentally validated. The assembled prototype machine along with a view of the rotor magnets and the fabricated PCB stator are shown in Fig. 9. The specifications and geometrical properties of the prototype are also provided in Table II. The SFF for the designed coils is 0.20, and the mechanical airgap was set to 1.3mm for the preliminary experiments. Accordingly, the current density was updated, and the corresponding DC copper loss is reported in Table III. The measurements and FEA results demonstrate a high level of consistency when considering the torque and back-EMF constants, as well as the phase resistance and inductance. The measured and FEA-based three-phase back-EMFs of the prototype machine are compared in Fig. 6, demonstrating a very good agreement.

TABLE II
Specifications and main dimensions of the selected design for prototyping.

Parameter	Value	Unit
Rated power	4.18	kW
Rated speed	2,100	rpm
Airgap (rotor to stator)	1.3	mm
Stator thickness	2.0	mm
Rotor outer diameter	304	mm
Rotor inner diameter	208	mm
Stator outer diameter	310	mm
Stator inner diameter	202	mm
No. of rotor poles	36	-
No. of stator coils	36	-

TABLE III
Experimentally measured the prototype machine parameters and power losses at the rated condition.

Parameter	Value	Unit
Torque constant	2.1	Nm/A
Phase resistance	0.8	Ω
Phase inductance	60.1	μH
DC copper losses	125.4	W
Eddy current losses	22.6	W
Circulating current losses	≤ 1	W
Mechanical losses	30.4	W
Efficiency	95.9	%

In order to measure the open circuit losses, several spindown tests were carried out, and mechanical losses are separated by repeating the tests with a dummy plastic stator. To separate the eddy and circulating current losses, the terminals of the four main parallel paths were brought out of the PCB stator, and the tests were repeated with and without connecting the parallel paths. Subtracting the measured losses gives the circulating current losses, as reported in Table III and demonstrated in Fig. 7. The eddy current losses at the rated speed are below 13% of the total rated losses, and the circulating current losses are below 1W, indicating the effectiveness of the proposed methods for loss reduction. The calculated efficiency at the rated condition is 95.9% which is above IE4 class according to the IEC/EN 60034 Standard.
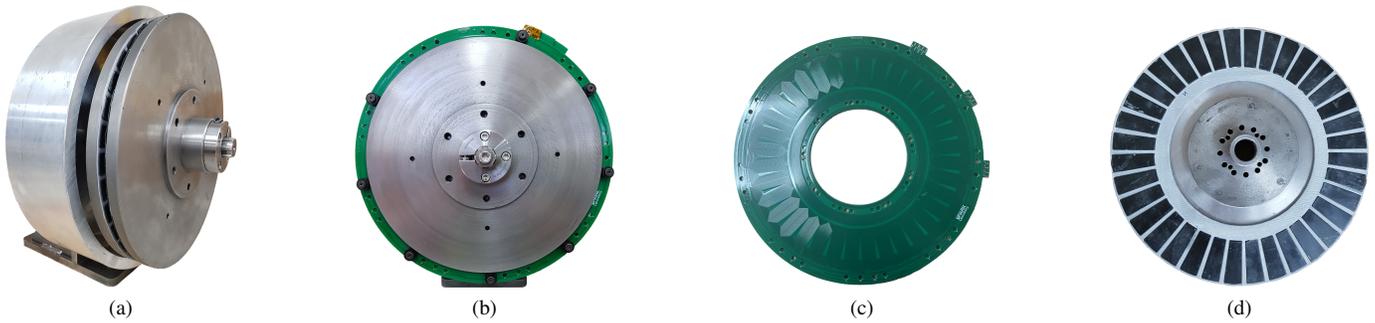
Fig. 9. The prototype three-phase double-rotor single-stator coreless axial flux PM machine with a rated torque of 19Nm at 2,100rpm (a). The assembled machine where the PCB stators are mounted on the machine hub (b). Three 36-pole PCB stators stacked together that are mechanically shifted by 6.66 degrees to form a 3-phase back-EMF (c). The 36-pole permanent magnet rotor with NdFeB PMs (d).

V. Conclusion

This paper presented the design of a highly efficient PCB stator coreless AFPM machine with minimal eddy and circulating current losses through a proposed multi-objective design optimization procedure. Different winding losses mitigation techniques were considered within this design procedure taking into account the PCB manufacturing limitations and standards. A prototype for the designed machine was built and the effectiveness of the proposed techniques and the optimization results were experimentally validated. The results demonstrated a very good agreement between simulation and measurement results and the machine efficiency is about 96% at the rated condition.

Acknowledgment

References

[1] F. Nishanth, J. Van Verdeghem, and E. L. Severson, "A review of axial flux permanent magnet machine technology," *IEEE Transactions on Industry Applications*, vol. 59, no. 4, pp. 3920–3933, 2023.

[2] F. Marcolini, G. De Donato, F. G. Capponi, M. Incurvati, and F. Caricchi, "Novel multiphysics design methodology for coreless axial flux permanent magnet machines," *IEEE Transactions on Industry Applications*, pp. 1–11, 2023.

[3] V. Rallabandi, N. Taran, D. M. Ionel, and J. F. Eastham, "Coreless multidisc axial flux pm machine with carbon nanotube windings," *IEEE Transactions on Magnetics*, vol. 53, no. 6, pp. 1–4, 2017.

[4] F. Copt, C. Koechli, and Y. Perriard, "Minimizing the circulating currents of a slotless bldc motor through winding reconfiguration," in *2015 IEEE Energy Conversion Congress and Exposition (ECCE)*, 2015, pp. 6497–6502.

[5] G. François and B. Dehez, "Impact of slit configuration on eddy current and supply current losses in PCB winding of slotless PM machines," *IEEE Transactions on Industry Applications*, vol. 58, no. 5, pp. 6035–6044, 2022.

[6] R. Wang and A. Kamper, "Evaluation of eddy current losses in axial flux permanent magnet (AFPM) machine with an ironless stator," in *Conference Record of the 2002 IEEE Industry Applications Conference. 37th IAS Annual Meeting (Cat. No.02CH37344)*, vol. 2, 2002, pp. 1289–1294 vol.2.

[7] Y. Chulaee, D. Lewis, A. Mohammadi, G. Heins, D. Patterson, and D. M. Ionel, "Circulating and eddy current losses in coreless axial flux PM machine stators with PCB windings," *IEEE Transactions on Industry Applications*, pp. 1–11, 2023.

[8] O. Taqavi and S. Mirimani, "Design aspects, winding arrangements and applications of printed circuit board motors: A comprehensive review," *IET Electric Power Applications*, vol. 14, pp. 1505–1518, 09 2020.

[9] F. Tokgöz, G. Çakal, and O. Keysan, "Comparison of PCB winding topologies for axial-flux permanent magnet synchronous machines," *IET Electric Power Applications*, 2020.

[10] A. Hembel and B. Sarlioglu, "PCB winding for electric machines with integrated 3d printed heat exchanger," in *2022 IEEE Transportation Electrification Conference Expo (ITEC)*, 2022, pp. 421–426.

[11] F. Marcolini, G. De Donato, F. G. Capponi, and F. Caricchi, "Design of a high speed printed circuit board coreless axial flux permanent magnet machine," in *2021 IEEE Energy Conversion Congress and Exposition (ECCE)*, 2021, pp. 4353–4360.

[12] B. Anvari, P. Guedes-Pinto, and R. Lee, "Dual rotor axial flux permanent magnet motor using PCB stator," in *2021 IEEE International Electric Machines Drives Conference (IEMDC)*, 2021, pp. 1–7.

[13] M. Rosu, P. Zhou, D. Lin, D. Ionel, M. Popescu, F. Blaabjerg, V. Rallabandi, and D. Staton, *"Multiphysics Simulation by Design for Electrical Machines, Power Electronics and Drives"*, J. Wiley - IEEE Press, 2017.

[14] *Ansys Electronics Desktop, Maxwell, version 23.1, 2023, ANSYS Inc.*

[15] N. Taran, V. Rallabandi, G. Heins, and D. M. Ionel, "Systematically exploring the effects of pole count on the performance and cost limits of ultrahigh efficiency fractional HP axial flux PM machines," *IEEE Transactions on Industry Applications*, vol. 56, no. 1, pp. 117–127, 2020.

[16] Y. Chulaee, D. Lewis, M. Vatani, J. F. Eashtam, and D. M. Ionel, "Torque and power capabilities of coreless axial flux machines with surface PMs and halbach array rotors," in *2023 IEEE International Electric Machines and Drives Conference (IEMDC)*, 2023, pp. 1–6.

[17] P. Han, D. Lawhorn, Y. Chulaee, D. Lewis, G. Heins, and D. M. Ionel, "Design optimization and experimental study of coreless axial-flux PM machines with wave winding PCB stators," in *2021 IEEE Energy Conversion Congress and Exposition (ECCE)*, 2021, pp. 4347–4352.

[18] D. Lawhorn, P. Han, D. Lewis, Y. Chulaee, and D. M. Ionel, "On the design of coreless permanent magnet machines for electric aircraft propulsion," in *2021 IEEE Transportation Electrification Conference Expo (ITEC)*, 2021, pp. 278–283.

[19] N. Taran, D. M. Ionel, V. Rallabandi, G. Heins, and D. Patterson, "An overview of methods and a new three-dimensional FEA and analytical hybrid technique for calculating AC winding losses in PM machines," *IEEE Transactions on Industry Applications*, vol. 57, no. 1, pp. 352–362, 2021.